

Report for exercise 4 from group I

Tasks addressed: 5
 Authors:
 Kejia Gao (03779844)
 Jingyi Zhang (03785924)
 Maximilian Mayr (03738789)
 Yizhi Liu (03779947)
 Felipe Antonio Diaz Laverde (03766289)
 Last compiled: 2024-06-09

The work on tasks was divided in the following way:

Kejia Gao (03779844)	Task 1	20%
	Task 2	20%
	Task 3	20%
	Task 4	20%
	Task 5	20%
Jingyi Zhang (03785924)	Task 1	20%
	Task 2	20%
	Task 3	20%
	Task 4	20%
	Task 5	20%
Maximilian Mayr (03738789)	Task 1	20%
	Task 2	20%
	Task 3	20%
	Task 4	20%
	Task 5	20%
Yizhi Liu (03779947)	Task 1	20%
	Task 2	20%
	Task 3	20%
	Task 4	20%
	Task 5	20%
Felipe Antonio Diaz Laverde (03766289)	Task 1	20%
	Task 2	20%
	Task 3	20%
	Task 4	20%
	Task 5	20%

1 TASK 1

Report on task TASK 1, Vector fields, orbits, and visualization

In order to create phase portraits for the linear system $\dot{\mathbf{x}} = \mathbf{A}_\alpha \mathbf{x}$ similar to those in Kuznetsov's book [2], we used the parametrized matrix

$$\mathbf{A}_\alpha = \begin{bmatrix} \alpha & \beta \\ |\beta| & \alpha \end{bmatrix}.$$

It can be computed that this matrix has the eigenvalues $\lambda_{1/2} = \alpha \pm \sqrt{\beta \cdot |\beta|}$. Further, we made the matrix only depend on one parameter by choosing $\beta = \alpha^3 - 3\alpha$. As a result of this choice, there are value ranges for α which lead to all five topological classes covered in Kuznetsov's book. These value ranges are listed in Table 1.

Topological class	Eigenvalues	Parameter constraints	Constraint for α
Stable node	Both real, negative	$0 < \beta < -\alpha$	$\alpha \in (-\sqrt{3}, -\sqrt{2})$
Stable focus	Complex conjugates, negative real part	$\alpha < 0, \beta < 0$	$\alpha < -\sqrt{3}$
Unstable saddle	Both real, one positive, one negative	$0 \leq \alpha < \beta$	$\alpha \in (-\sqrt{2}, 0) \cup (2, \infty)$
Unstable node	Both real, positive	$0 < \beta < \alpha$	$\alpha \in (\sqrt{3}, 2)$
Unstable focus	Complex conjugates, positive real part	$\alpha > 0, \beta < 0$	$\alpha \in (0, \sqrt{3})$

Table 1: Constraints for the parameter to be in a topological class

Figure 1 shows one phase portrait for each topological class in the form of a streamplot with one exemplary trajectory plotted in orange. The parameters used are shown in the respective captions.

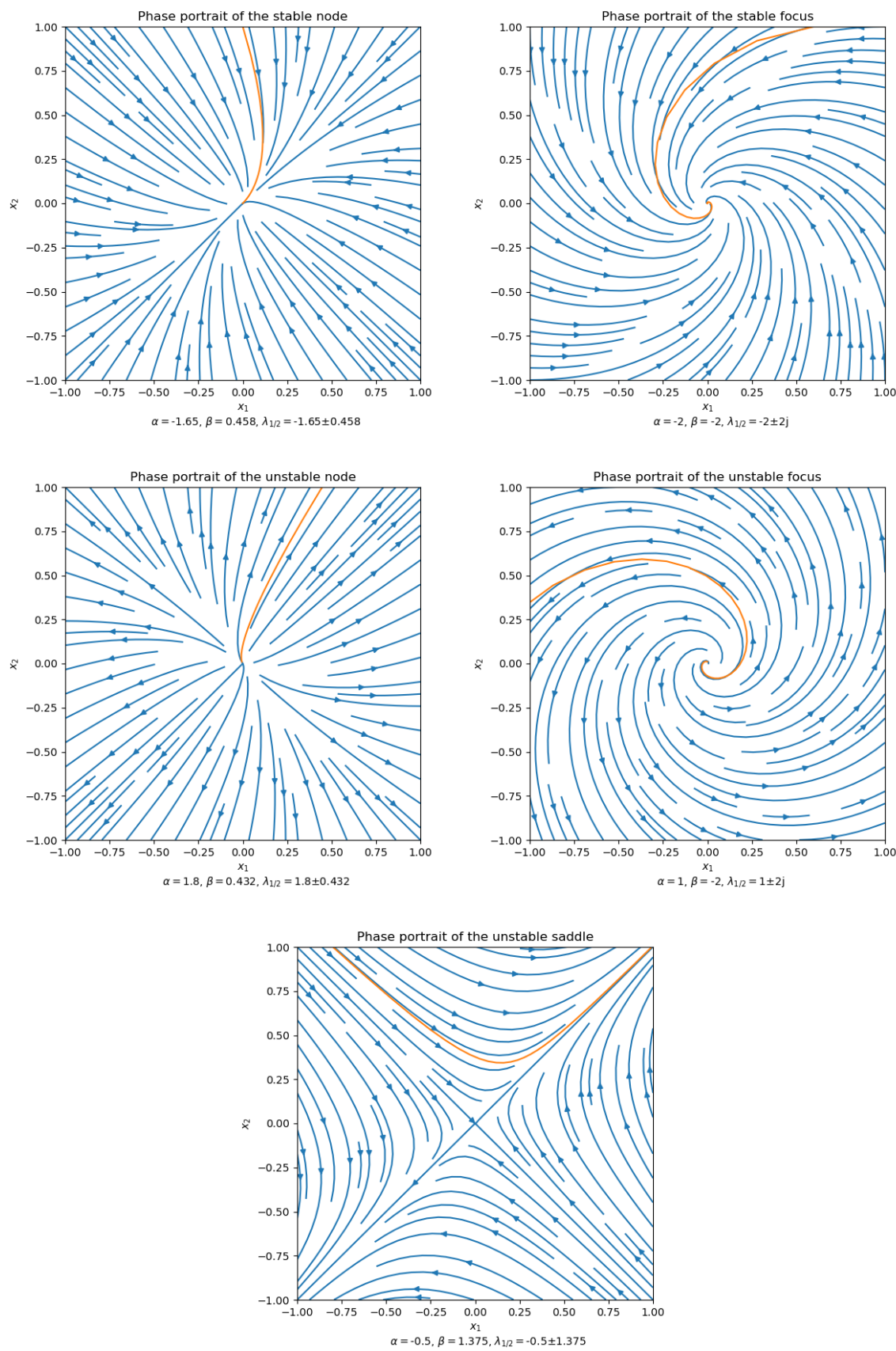


Figure 1: Phase portraits for all five topological classes

The systems resulting in nodes and foci of the same stability are topologically equivalent because there exists a homeomorphism transforming the orbit of the node system to this of a focus system with the same stability and vice versa while preserving the direction of time. This homeomorphism can be described as follows. Since both versions share the same steady state at $(0, 0)$, these can easily be mapped to each other without transformation. In a system with a node, the remaining points move over time in a relatively straight line from or to the steady state depending on the stability, whereas they move on spiral trajectories for foci. Visually speaking, the transformation rotates the phase portraits with a larger rotation the closer the distance to the steady state. So, the transformation from a node to a focus rolls the relatively straight trajectory to a spiral while the reverse transformation unrolls it. Only the nodes and foci of the same stability are topologically equivalent because otherwise the direction of time would change as can be seen in Figure 1. A formal proof can be found in Kuznetsov's book. [2]

2 TASK 2

Report on task TASK 2, Common bifurcations in nonlinear systems

In this report, we analyze two nonlinear dynamical systems given by:

$$\begin{aligned}\dot{x} &= \alpha - x^2 \quad (\text{System1}) \\ \dot{x} &= \alpha - 2x^2 - 3 \quad (\text{System2})\end{aligned}\tag{1}$$

We aim to determine the types of bifurcations occurring in these systems as the parameter α varies, plot their bifurcation diagrams, and evaluate the stability of the steady states. Additionally, we will discuss whether these systems are topologically equivalent for certain values of α and provide arguments for their normal form equivalence.

2.1 System 1

Bifurcation at $\alpha = 0$

For $\alpha > 0$, the system has two steady states at $x_0 = \pm\sqrt{\alpha}$.

For $\alpha < 0$, there are no steady states.

At $\alpha = 0$, the system undergoes a saddle-node bifurcation, where two steady states collide and annihilate each other.

The bifurcation diagram for system 1 is shown below, where the solid lines represent stable steady states and the dashed lines represent unstable steady states.

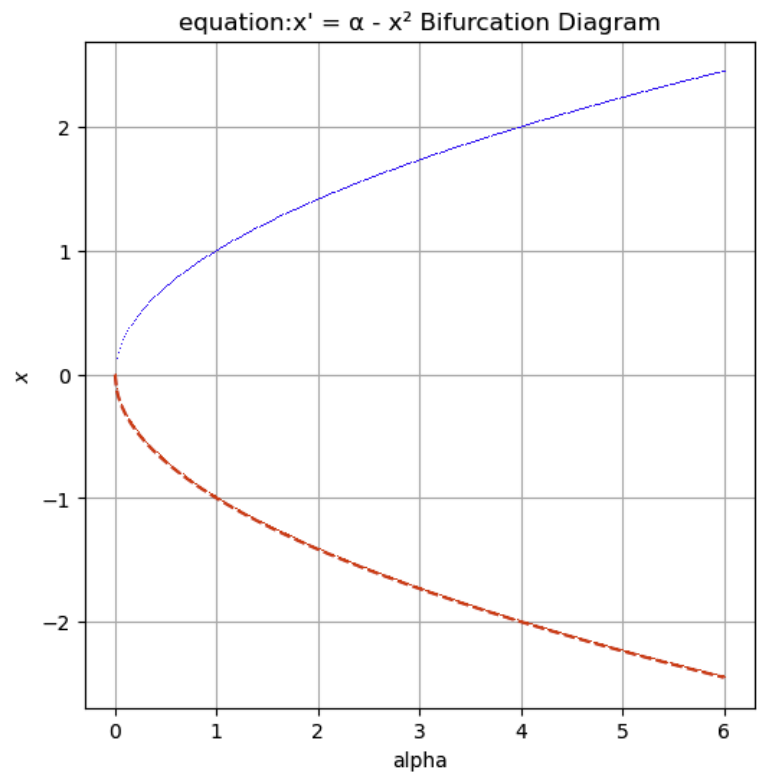


Figure 2: Bifurcation Diagram: System 1

The bifurcation diagram illustrates the behavior of the dynamical system 1 as the parameter α varies from -0.5 to 1.5. The x-axis represents the parameter α , while the y-axis represents the steady states of the system. As the parameter α increases, the system initially has a single stable equilibrium point. When α reaches a critical value, the system undergoes a bifurcation, resulting in the creation of two new equilibrium points. One of these points is stable (shown in solid blue), and the other is unstable (shown in dashed red). This behavior is characteristic of a saddle-node bifurcation, where the system transitions from a single equilibrium to multiple equilibria as the parameter α changes.

2.2 System 2

The dynamical system is given by:

$$\dot{x} = \alpha - 2x^2 - 3$$

We analyze the system's behavior for different values of α : For $\alpha > 3$, in this regime, there are two steady states at $x = \pm \sqrt{\frac{\alpha-3}{2}}$. These states are determined by setting $\dot{x} = 0$. Here, $x = \sqrt{\frac{\alpha-3}{2}}$ is a stable equilibrium, while $x = -\sqrt{\frac{\alpha-3}{2}}$ is an unstable equilibrium.

At $\alpha = 3$, the system has a semi-stable equilibrium point (saddle point) located at $x = 0$.

When $\alpha < 3$, there are no real equilibrium states.

The bifurcation diagram for system 2 is shown below. Because the form of System 2 and System 1 is similar, the resulting graphs are also similar. By comparison, the change of the stable state x with alpha in System 2 is slower than that in System 1, because the coefficient before the square term of x changes.

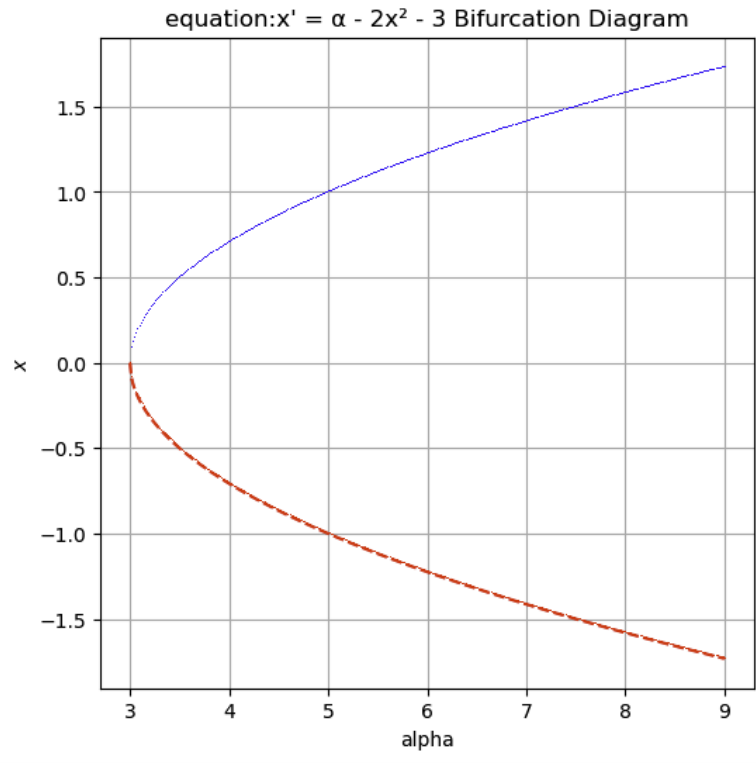


Figure 3: Bifurcation Diagram: System 2

2.3 Topological Equivalence

At $\alpha = 1$, the first system $\dot{x} = \alpha - x^2$ has two fixed points: $x = 1$ and $x = -1$. The fixed point at $x = 1$ is stable (attractive), while the fixed point at $x = -1$ is unstable (repulsive). This indicates that the system has distinct regions of attraction and repulsion. On the other hand, the second system $\dot{x} = \alpha - 2x^2 - 3$ has no fixed points, as there are no real solutions to the equation $\alpha - 2x^2 - 3 = 0$ when $\alpha = 1$. Consequently, the phase portraits of these two systems are fundamentally different, as one exhibits fixed points with associated stability properties, while the other does not. Therefore, the two systems are not topologically equivalent at $\alpha = 1$.

At $\alpha = -1$, both the first system $\dot{x} = \alpha - x^2$ and the second system $\dot{x} = \alpha - 2x^2 - 3$ have no fixed points because the equations $\alpha - x^2 = 0$ and $\alpha - 2x^2 - 3 = 0$ yield no real solutions for $\alpha = -1$. In this scenario, the trajectories for both systems will always move away from any initial condition towards negative infinity, indicating that both systems exhibit similar qualitative behavior with trajectories moving away from the origin. Since both systems lack fixed points and their trajectories qualitatively behave in the same manner, they exhibit similar overall dynamics. As a result, the systems are likely to be topologically equivalent at $\alpha = -1$.

2.4 Normal Form Argument

To formally argue that both systems have the same normal form, consider that:

Canonical Form: Both systems can be written in the form involving a dominant quadratic term and a constant term, i.e.,

$$\dot{x} = \alpha - kx^2 - c,$$

where k and c are constants.

Scaling and Transformation: Through appropriate scaling (multiplication by constants) and translations, both systems can be reduced to a comparable form, indicating they share the same normal form.

3 TASK 3

Report on task TASK 3, Bifurcations in higher dimensions

3.1 Andronov-Hopf Bifurcation

3.1.1 Phase Portraits

Andronov-Hopf bifurcation is a two-dimensional system defined as Equation 2. To visualize the phase portraits, the first step is to set up Numpy arrays for grid coordinates. For every grid point, calculate the two-dimensional gradient via Equation 2. A function called “streamplot” is used to plot the phase portraits. As Figure 4 displays, the phase portrait varies with the value of α . If $\alpha < 0$, trajectories converge to the origin, indicating a stable focus. If $\alpha = 0$, there exist closed orbits and the fixed point at the origin is marginally stable. If $\alpha > 0$, the fixed point at the origin is unstable and a limit cycle surrounds the origin.

$$\begin{aligned}\dot{x}_1 &= \alpha x_1 - x_2 - x_1(x_1^2 + x_2^2), \\ \dot{x}_2 &= x_1 + \alpha x_2 - x_2(x_1^2 + x_2^2)\end{aligned}\tag{2}$$

3.1.2 Orbits

The function `plot_orbits` is used to plot the orbits. For a specified system given α and `init_state` : $(x_1^{(0)}, x_2^{(0)})$, use the system function (Equation 2) to compute the gradient $(\dot{x}_1^{(0)}, \dot{x}_2^{(0)})$. According to Euler’s method, the next state is calculated by adding $(x_1^{(n)}, x_2^{(n)}) = (x_1^{(n-1)}, x_2^{(n-1)}) + \Delta t \cdot (\dot{x}_1^{(n-1)}, \dot{x}_2^{(n-1)})$, $n \in \mathbb{N}^*$. Iterate the function for 2000 times with $\Delta t = 0.005s$ and store the data of $(x_1^{(i)}, x_2^{(i)})$, $i \leq 2000$, $i \in \mathbb{N}$ into the Numpy array named `trajectory_matrix`, which can be used to plot the orbits.

The results are shown in Figure 5. If the starting point is $(2, 0)$, the orbit looks like σ . At first, the orbit is a curve outside the unit circle centered at the origin. Afterwards, it becomes that unit circle. If the starting point is $(0.5, 0)$, the orbit is a curve inside the unit circle and is then transformed into the unit circle.

3.2 Cusp Bifurcation

Cusp bifurcation is defined by Equation 3. To plot the 3D surface, sample points (x, α_2) uniformly. In the setup, both x and α_2 have 200000 data points ranging from $[-3, 3]$. Set $\dot{x} = 0$, then we get $\alpha_1 = -\alpha_2 x + x^3$. Afterwards, the 3D surface (α_1, α_2, x) can be plotted via the function named `ax.scatter()`.

$$\dot{x} = \alpha_1 + \alpha_2 x - x^3\tag{3}$$

Equation 3 illustrates the 3D surface of the cusp bifurcation. The cusp point is where the system undergoes a transition, causing a dramatic change in behavior. The shape of the bifurcation surface around the cusp point looks like the pointed end where two curves meet, which explains why it is called cusp bifurcation.

4 TASK 4

Report on task TASK 4, Chaotic dynamics

4.1 Part 1 Logistic map

4.1.1 Theoretical analysis

Logistic map is a discrete system defined by Equation 4. In Part 1, it is required to find out the system behavior with regard to the parameter r , with $r \in (0, 4]$, $x \in [0, 1]$.

$$x_{n+1} = rx_n(1 - x_n), n \in \mathbb{N}\tag{4}$$

Suppose that the logistic map is represented by Equation 5.

$$f(x) = rx(1 - x)\tag{5}$$

The derivative of $f(x)$ is notated as $f'(x)$, as Equation 6 shows.

$$f'(x) = r(1 - 2x)\tag{6}$$

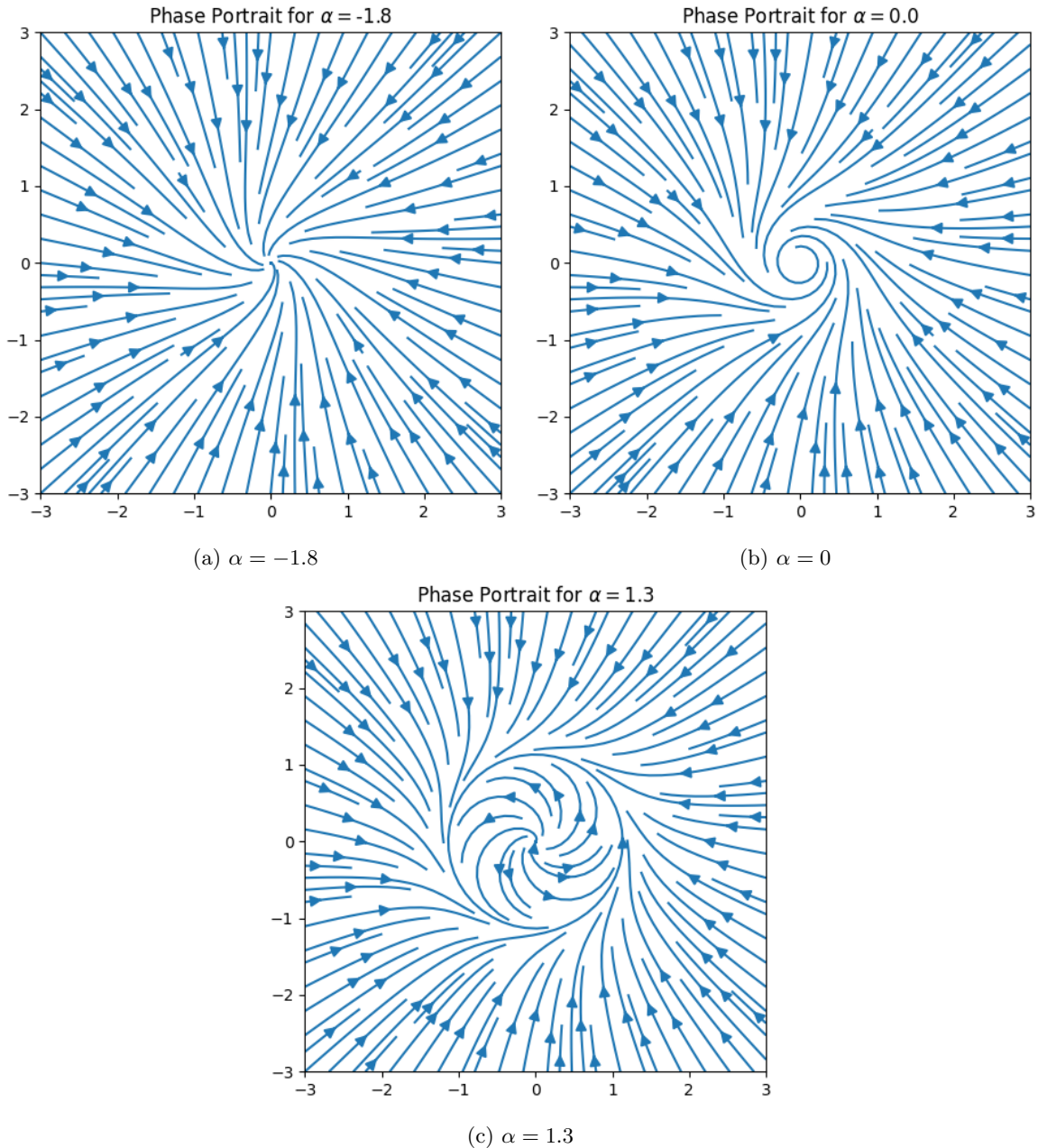


Figure 4: Phase portraits of Andronov-Hopf Bifurcation

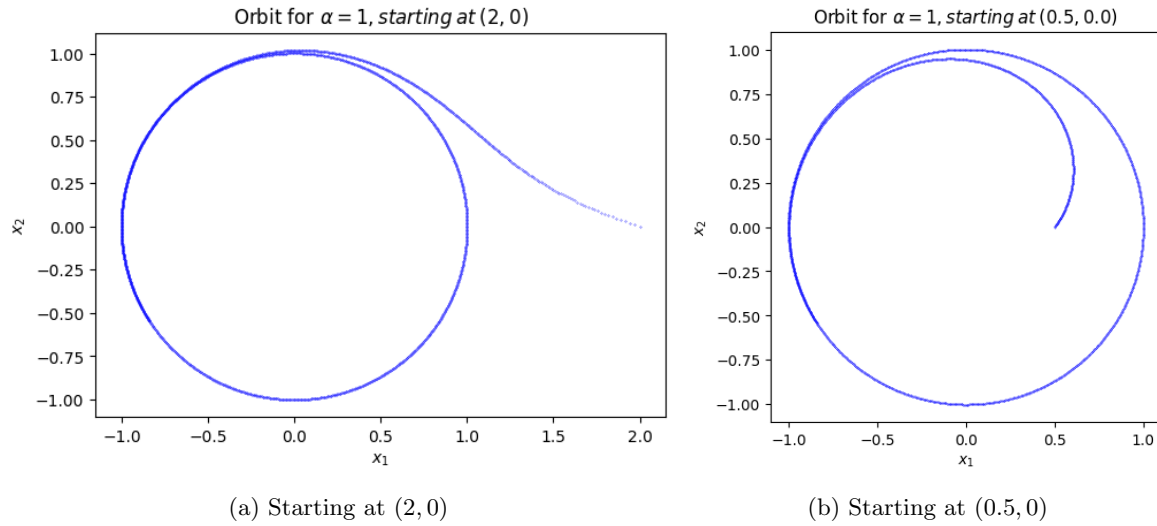


Figure 5: Orbits of Andronov-Hopf Bifurcation

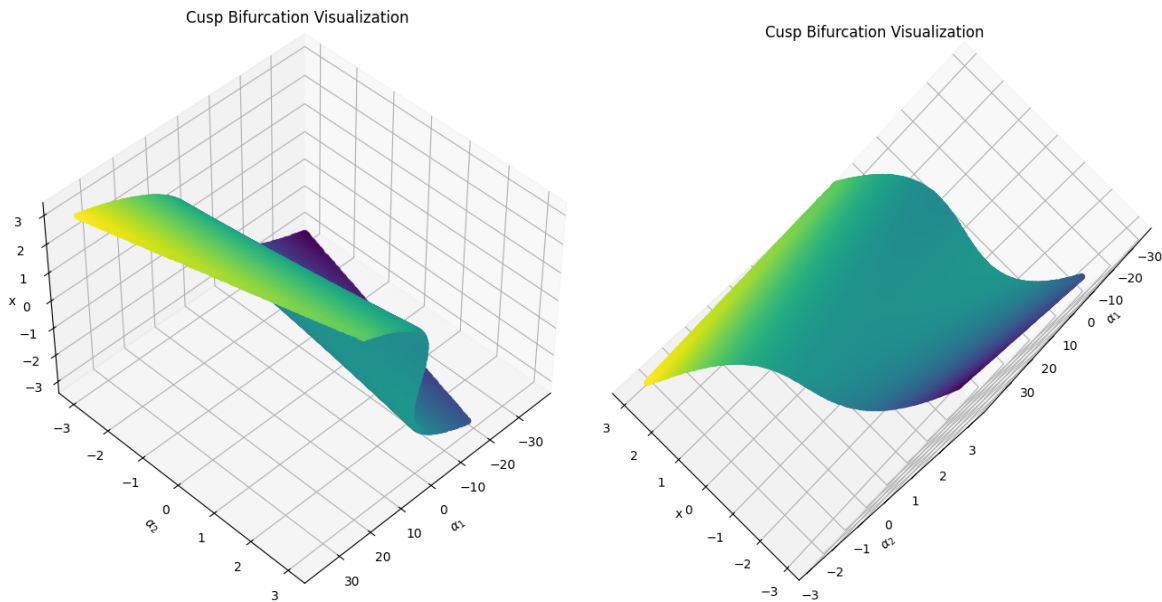


Figure 6: Bifurcation surface of the cusp bifurcation

x_{ss} is the steady state, which is computed by Equation 7.

$$f(x_{ss}) = rx_{ss}(1 - x_{ss}) = x_{ss} \quad (7)$$

Solve the equation. We get $x_{ss,1} = 0$ and $x_{ss,2} = 1 - \frac{1}{r}$.

There are 3 cases related to system stability[3]:

1. If $|f'(x_{ss})| < 1$, then $|x_{n+1}| < |x_n|$, the value is convergent and the fixed point is thus stable.
2. If $|f'(x_{ss})| > 1$, then $|x_{n+1}| > |x_n|$, the value is divergent and the fixed point is thus unstable.
3. If $|f'(x_{ss})| = 1$, then $|x_{n+1}| = |x_n|$, the stability is not determinate to linear order.

The conclusions can be applied to this specific problem.

- 1) If $x_{ss} = x_{ss,1} = 0$, then $f'(x_{ss}) = r$. To get a stable fixed point, $|r| < 1$. Combined with the problem description, we get $0 < r < 1$.
- 2) If $x_{ss} = x_{ss,2} = 1 - \frac{1}{r}$, then $f'(x_{ss}) = 2 - r$. To get a stable fixed point, $|2 - r| < 1$. Combined with the problem description, we get $1 < r < 3$.
- 3) If $r = 1$, $x_{ss} = x_{ss,1} = x_{ss,2} = 0$ and $f'(x_{ss}) = 1$. The fixed point is marginally stable.
- 4) If $r = 3$, $x_{ss,1} = 0$ and $x_{ss,2} = \frac{2}{3}$. and $f'(x_{ss}) = 1$. For the first fixed point $x_{ss,1} = 0$, $f'(x_{ss,1}) = 3 > 1$, which means it is unstable. For the second fixed point $x_{ss,2} = \frac{2}{3}$, $f'(x_{ss,2}) = -1$, which is a more complicated situation related to a period-doubling bifurcation and will be shown in the visualization of the simulation.
- 5) If $3 < r \leq 4$, $f'(x_{ss,1}) = r > 1$ and $f'(x_{ss,2}) = 2 - r < -1$. There is no stable point. The system has more complicated behavior.

4.1.2 Vary r from 0 to 2

The state value x of the system is calculated with the variable $r = 0.5, 1, 1.5$ and 2 , as Figure 7 demonstrates.

The cases where the initial value $x_0 = 0$ or 1 are analyzed separately because x_1 is 0 in the next state and x_n remains to be 0 in the following iterations.

For $x_0 = 0.2, 0.4, 0.6, 0.8$, when $r = 0.5$, x_n converges to 0 within a few iterations regardless of initial values. When $r = 1$, x_n converges to 0 slowly due to marginal stability. When $r = 1.5$, x_n converges to $x_{ss} = 1 - \frac{1}{r} = \frac{1}{3}$ within a few iterations. Similarly, when $r = 2$, the steady state is $x_{ss} = 0.5$.

4.1.3 Vary r from 2 to 4

The state value x of the system is calculated with the variable $r = 2.5, 3, 3.25, 3.5, 3.75$ and 4 (see Figure 8).

In the same way, if $x_0 = 0$ or 1 , x_n converges to 0 after the first iteration.

For other initial values $x_0 = 0.2, 0.4, 0.6, 0.8$, when $r = 2.5$, x_n converges to 0.6 within a few iterations regardless of initial values. But the system behavior becomes more and more complicated if r reaches 3 and continues to increase.

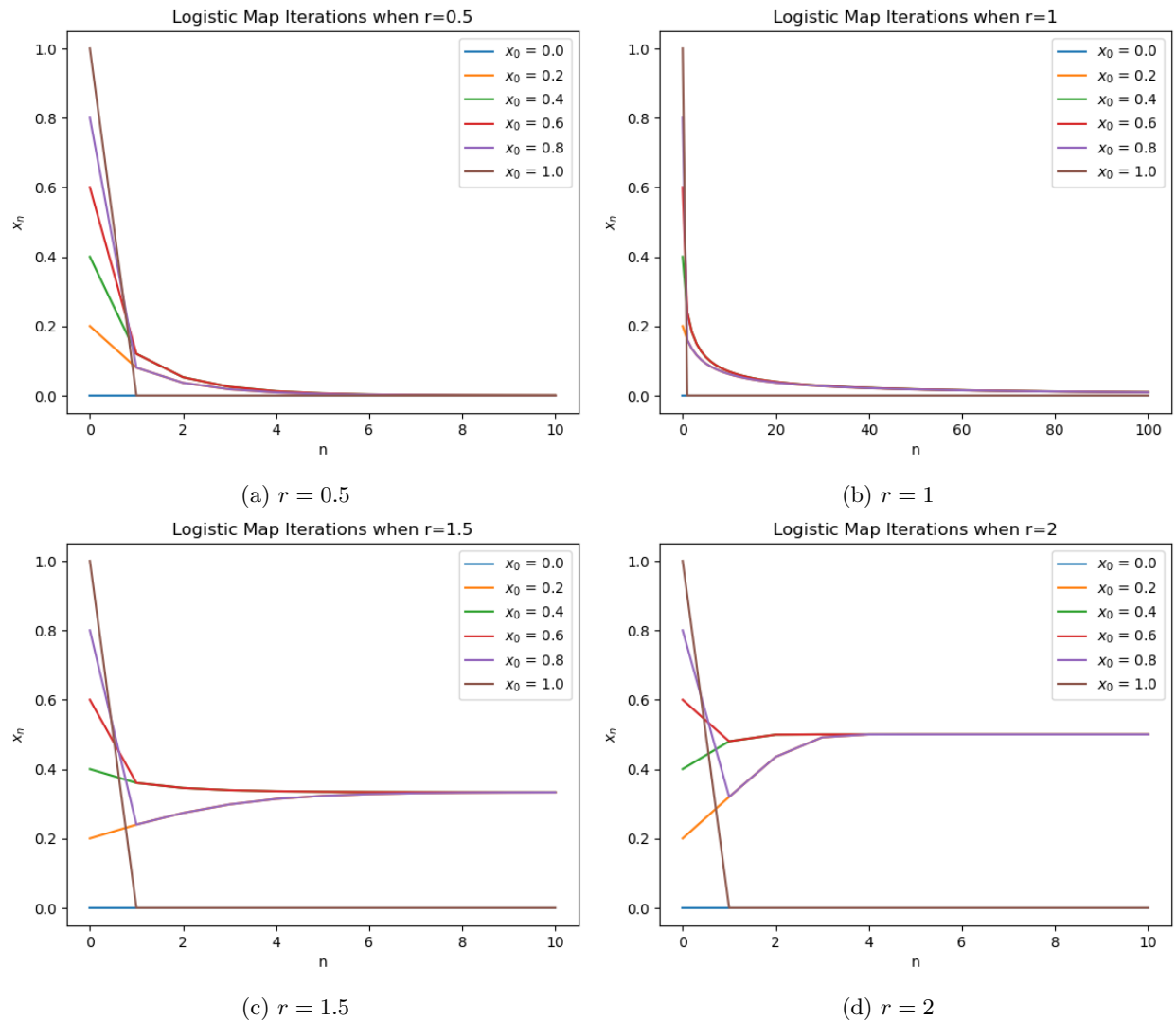
When $r = 3$, x_n shows periodicity approximately with $period = 2$, because x_n oscillates between 2 values (0.69 and 0.64) and the peak value decreases slightly as the iteration proceeds, while the valley value increases slightly. The peak value and valley value keep getting closer slowly but the oscillation continues to remain.

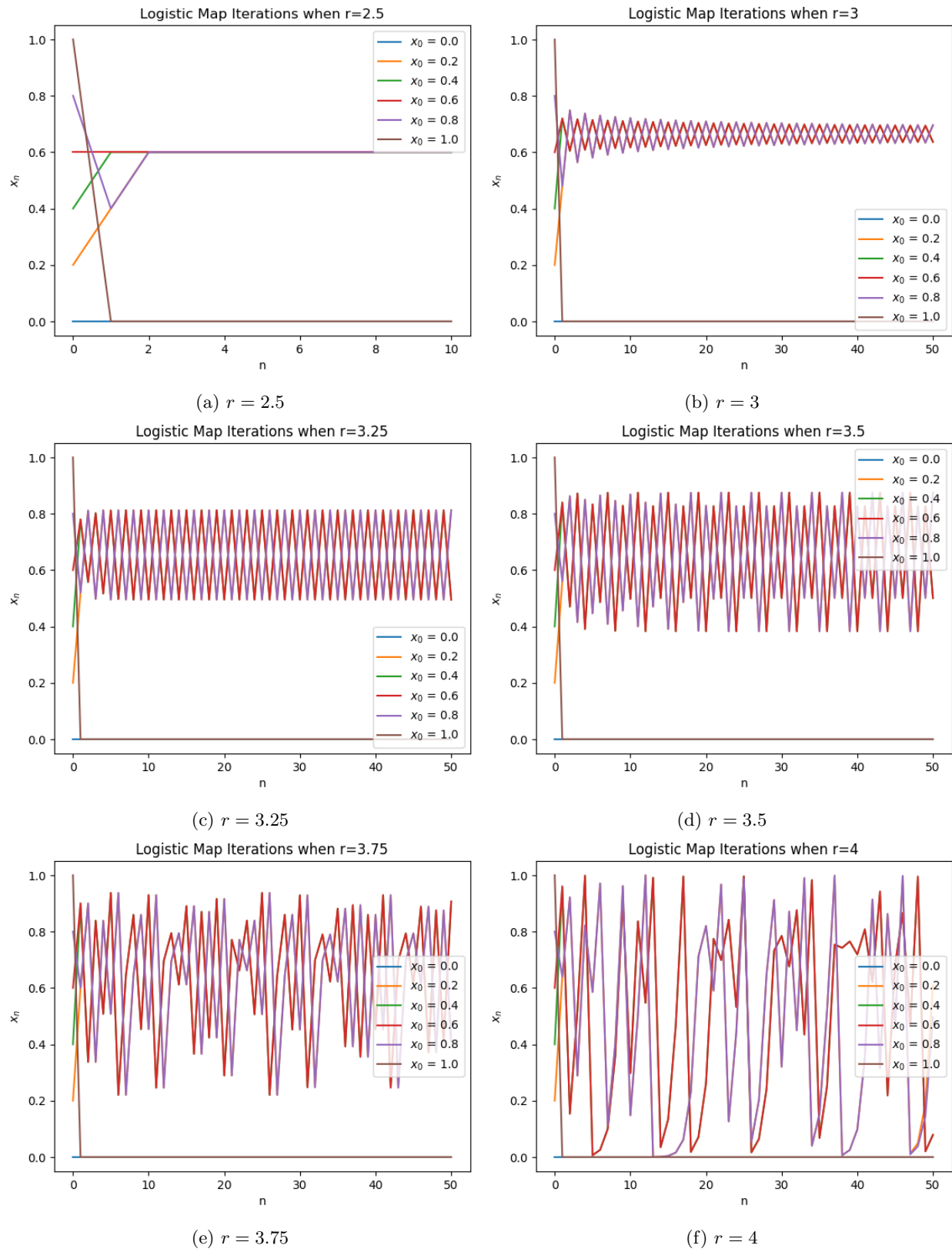
When $r = 3.25$, x_n has periodicity with $period = 2$ after 15 iterations. The peak value (0.81242714) and valley value (0.49526517) don't change anymore.

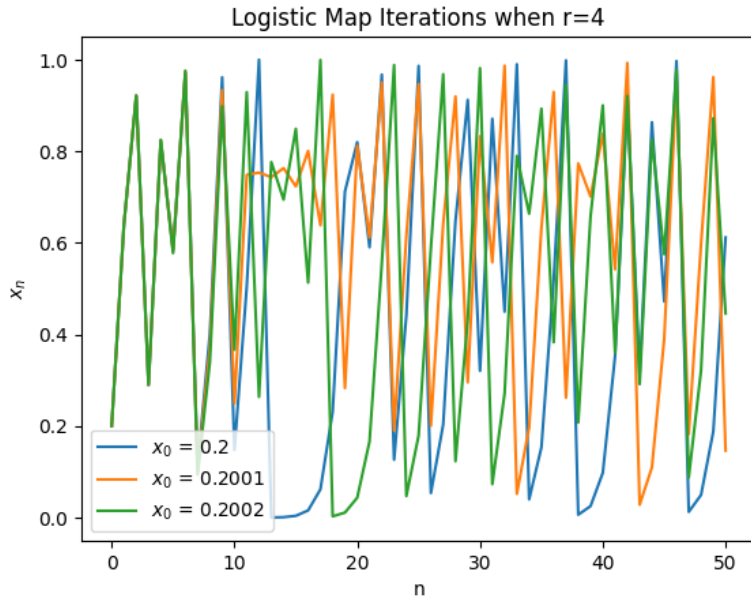
When $r = 3.5$, x_n has periodicity with $period = 4$ after 34 iterations. The 4 covered values (0.87499726 , 0.38281968 , 0.82694071 and 0.50088421) remain unchanged with the iteration.

When $r = 3.75$, x_n shows no obvious periodicity even when we check the values of 1000 iterations. There are narrow windows where the system temporarily exhibits approximate periodic behavior. Therefore, the system is unpredictable.

When $r = 4$, x_n has no periodicity at all, even without temporary and approximate periodic behavior. It is extremely sensitive to initial values, because even a slight change of the initial value will cause completely different system behavior, as Figure 9 illustrates. Therefore, the system is fully chaotic if $r = 4$.

Figure 7: Logistic map iteration with r from 0 to 2

Figure 8: Logistic map iteration with r from 2 to 4

Figure 9: System's sensitivity to initial values when $r = 4$

4.1.4 Bifurcation diagram for r between 0 and 4

The bifurcation diagram is in Figure 10. The result is consistent with the visualizations in Figure 7 and Figure 8. When $0 < r < 1$, the steady state is $x_{ss} = 0$ and the system is stable. When $r = 1$, the steady state is $x_{ss} = 0$ but it takes more iterations to converge to 0, since the system is marginally stable. When $1 < r < 3$, the steady state is $x_{ss} = 1 - \frac{1}{r}$ and the system is stable. When $r = 3$, the steady state is $x_{ss} = \frac{2}{3}$ but x_n oscillates around $\frac{2}{3}$ between two values a and b ($a < \frac{2}{3} < b$ with a increasing and b decreasing slightly), since the system is marginally stable. When $3 < r \lesssim 3.45$, there is no steady state and x_n oscillates between 2 values. When $3.45 < r \lesssim 3.54$, there is no steady state and x_n oscillates among 4 values with a period of 4. When $3.54 < r \lesssim 4$, there may exist periodicity but in most cases it is unpredictable[5]. When $r = 4$, the system is completely chaotic.

4.2 Part 2 Lorenz attractor

The Lorenz attractor is a three-dimensional dynamical system resulting in chaotic dynamics. It is defined by Equation 8. For this task, the parameters σ and β are fixed as $\sigma = 10$ and $\beta = \frac{8}{3}$. We analyze the system for two different values for ρ and show the influence of a small variation in the starting position on the resulting trajectory.

$$\begin{aligned}\dot{x}_1 &= \sigma(x_2 - x_1) \\ \dot{x}_2 &= x_1(\rho - x_3) - x_2 \\ \dot{x}_3 &= x_1x_2 - \beta x_3\end{aligned}\tag{8}$$

4.2.1 Strange attractor ($\rho = 28$)

Figure 11 shows the trajectory with a starting position $\mathbf{x}_0 = (10, 10, 10)$ within $T = 1000$ time units. The trajectory is computed with Euler's algorithm and a time step size of $\Delta t = 0.01$. It can be seen that the trajectory circles around two different steady states (visually speaking, in the center of the butterfly's wings) and switches between the steady states in the process. However, the trajectory never converges to either steady state during the simulated time. There is actually another (unstable) steady state at $\mathbf{0}$ since naturally a trajectory with the starting position $\mathbf{x}_0 = \mathbf{0}$ will never leave the origin. Trajectories with other initial positions might converge to the origin as well. For instance, all starting positions on the z-axis lead to this behavior.

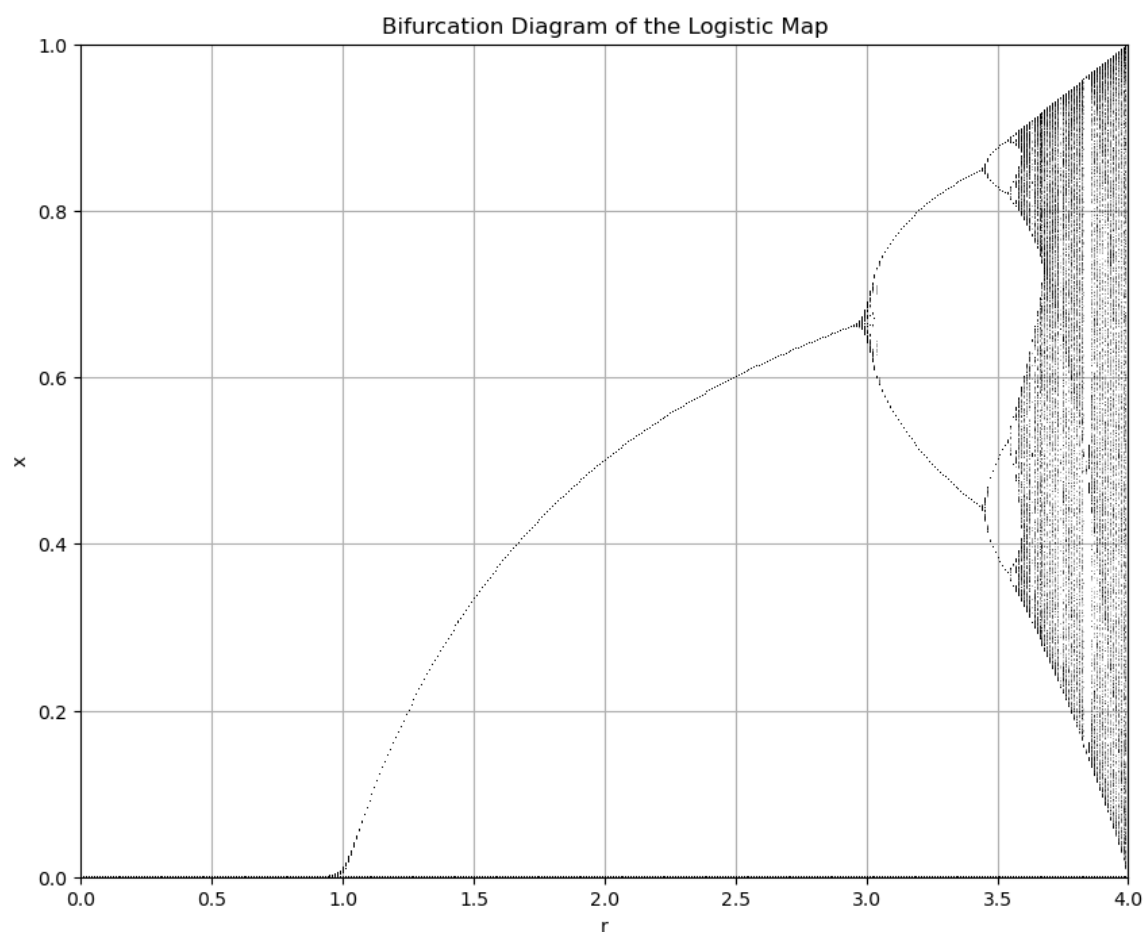
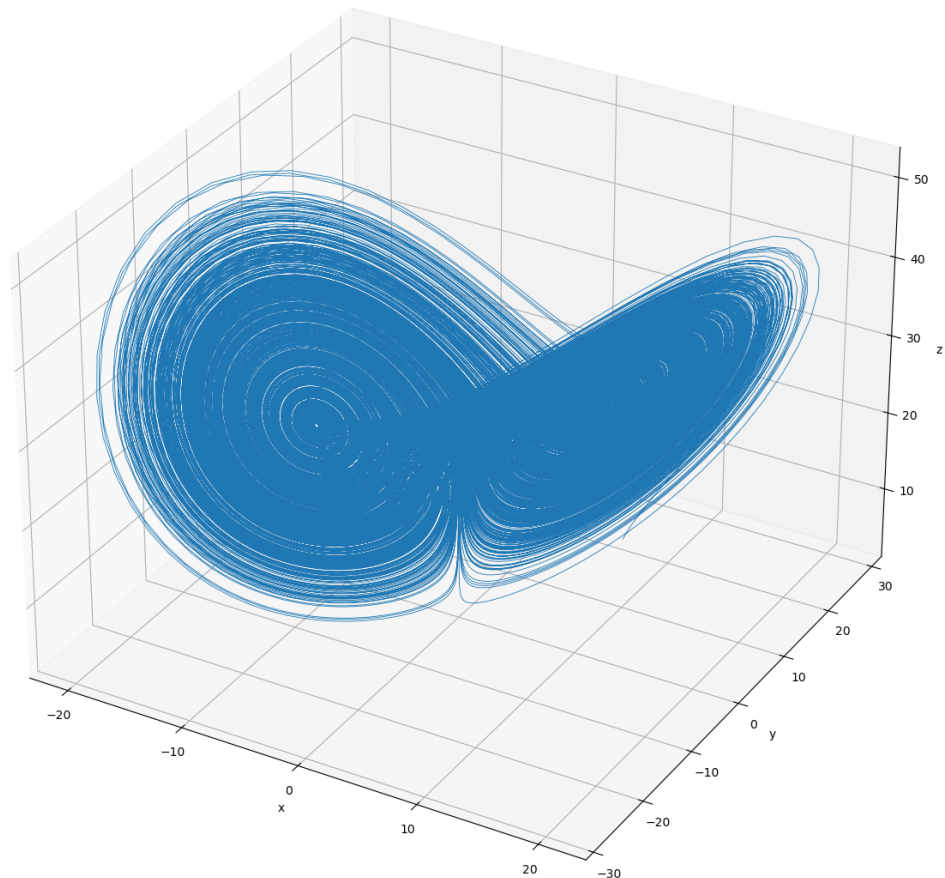


Figure 10: Bifurcation diagram of logistic map

Lorenz attractor with $\sigma = 10$, $\beta = 2.667$, $\rho = 28$, and without noiseFigure 11: Trajectory of the Lorenz attractor with $\rho = 28$ and $\mathbf{x}_0 = (10, 10, 10)$

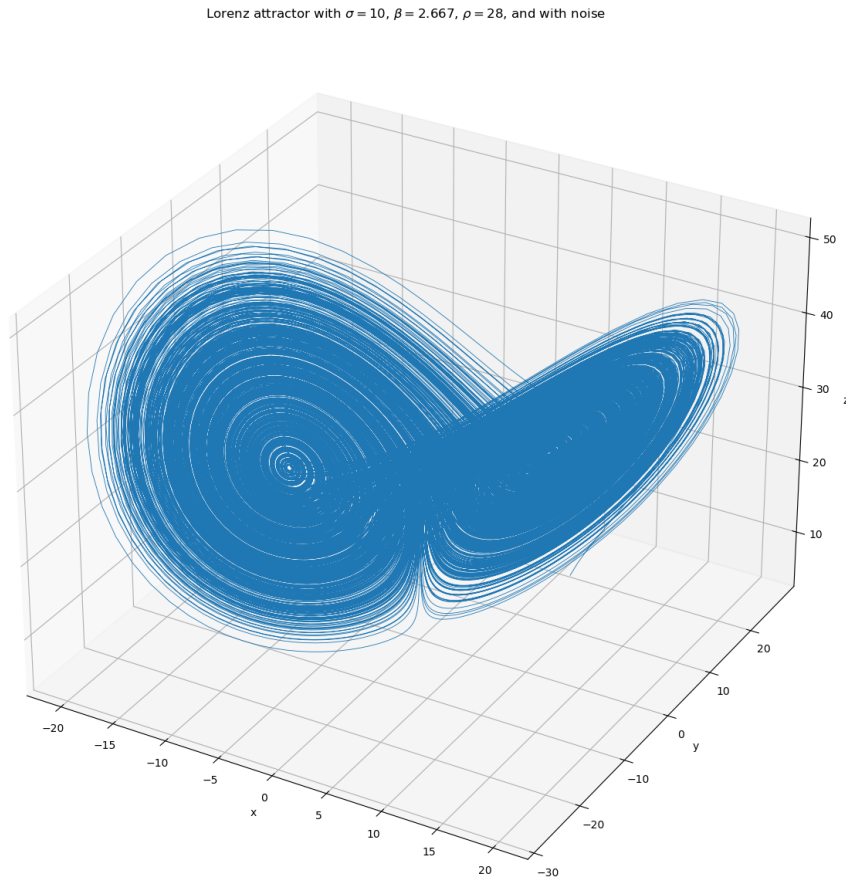


Figure 12: Trajectory of the Lorenz attractor with $\rho = 28$ and $\mathbf{x}_0 = (10 + 10^{-8}, 10, 10)$

4.2.2 The effect of noise

Figure 12 shows the trajectory for the same Lorenz attractor with a slightly modified starting position. The x-coordinate is changed by a difference of 10^{-8} . This can be interpreted as adding noise to the input. On first glance, the trajectories for the two different starting locations do not seem to differ drastically.

However, only the final orbits resemble each other while the distance between the actual positions at any given time might be up to the diameter of the entire orbit. This is illustrated in Figure 13. The system's chaotic nature leads to errors growing exponentially over time. For the chosen values, the error (squared distance) is initially 10^{-16} but after only 2071 time seps (of 100000 total) or 20.71 time units, the error raises over 1. Even before the first 100 time units pass, the error reaches relatively high values. For the remainder of the simulation, the error seems to be arbitrary because the trajectories are completely different by now. As a result, the positions for a given point in time might be on the completely opposite site of the orbit but could also, coincidentally, be almost equal (which is of course much less likely).

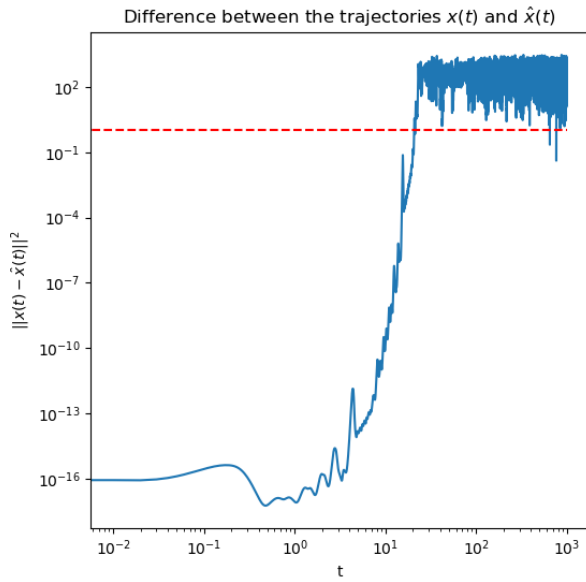


Figure 13: Squared distance between the trajectories for $\rho = 28$ over time. The red line marks a Euclidean distance of 1.

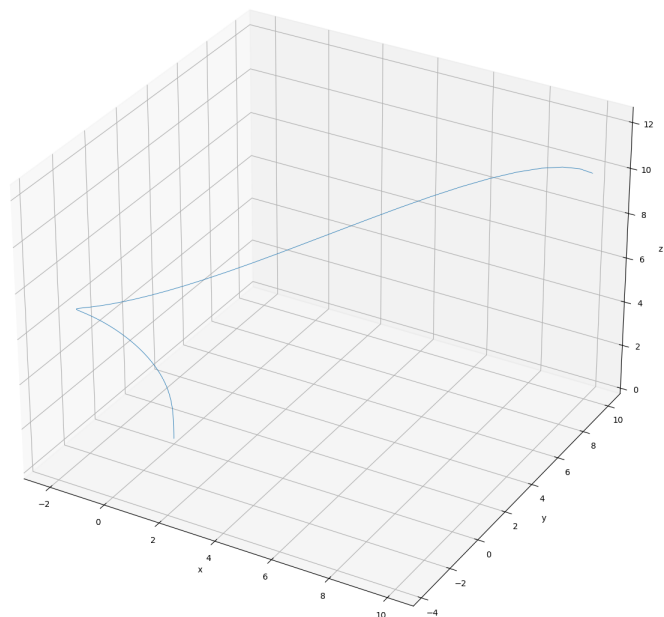
4.2.3 Stable attractor ($\rho = 0.5$)

For this section, we changed the parameter ρ to the value 0.5 and conducted the same experiments as above. Figure 14 shows the trajectory for the original initial position, Figure 15 the trajectory for the noisy starting position, and Figure 16 the error caused by the noisy input.

Both trajectories converge to the stable steady state in the origin and again, they look pretty similar. However, this time there is no chaos but stability in the system. Thus, the trajectories do not only look similar but are actually similar this time. This can also be concluded from the vanishing error. In contrast to the strange attractor before, there is no exponential growth of the error but an exponential decay. Hence, the original error of 10^{-16} is the highest error value during the entire simulation.

This change in behavior is caused by multiple bifurcations. It can be argued that there has to be at least one bifurcation for 2 reasons. On the one hand, the two steady states the trajectory circled around do not exist for $\rho = 0.5$ and on the other hand, the steady state in the origin is stable whereas it was unstable for $\rho = 28$.

According to Doedel et al. [1] several bifurcations happen. A bifurcation diagram is displayed in Figure 17. It shows that at $\rho = 1$ a pitchfork bifurcation happens. As a result, there are 2 additional stable steady states referred to as p^+ and p^- (the centers of the butterfly's wings), and the steady state in the origin becomes unstable. At $\rho \approx 13.9265$ a homoclinic bifurcation and at $\rho \approx 24.0579$ a heteroclinic connection happens. Finally, at $\rho \approx 24.7368$ a Hopf bifurcation happens, which leads to p^+ and p^- becoming unstable and triggering the occurrence of saddle foci (which lead to orbits looking like butterflies and the system not converging).

Lorenz attractor with $\sigma = 10$, $\beta = 2.667$, $\rho = 0.5$, and without noiseFigure 14: Trajectory of the Lorenz attractor with $\rho = 0.5$ and $\mathbf{x}_0 = (10, 10, 10)$

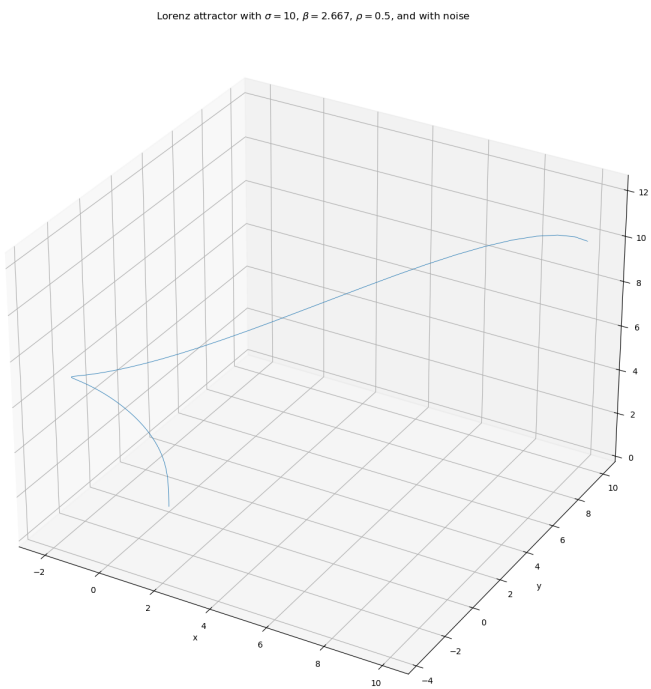


Figure 15: Trajectory of the Lorenz attractor with $\rho = 0.5$ and $\mathbf{x}_0 = (10 + 10^{-8}, 10, 10)$

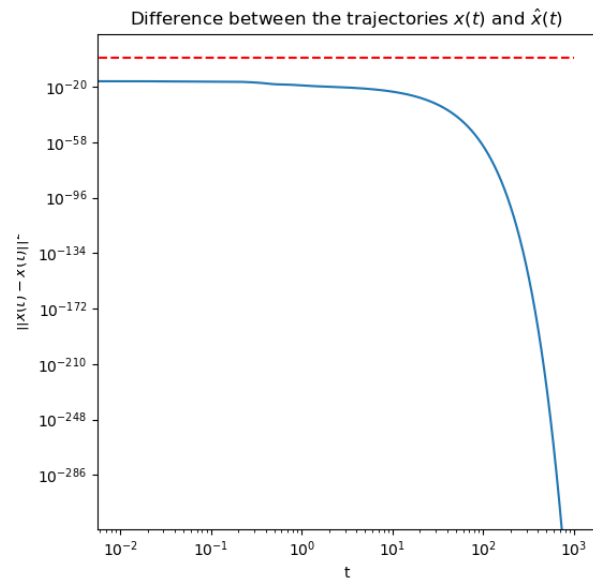


Figure 16: Squared distance between the trajectories for $\rho = 0.5$ over time. The red line marks a Euclidean distance of 1.

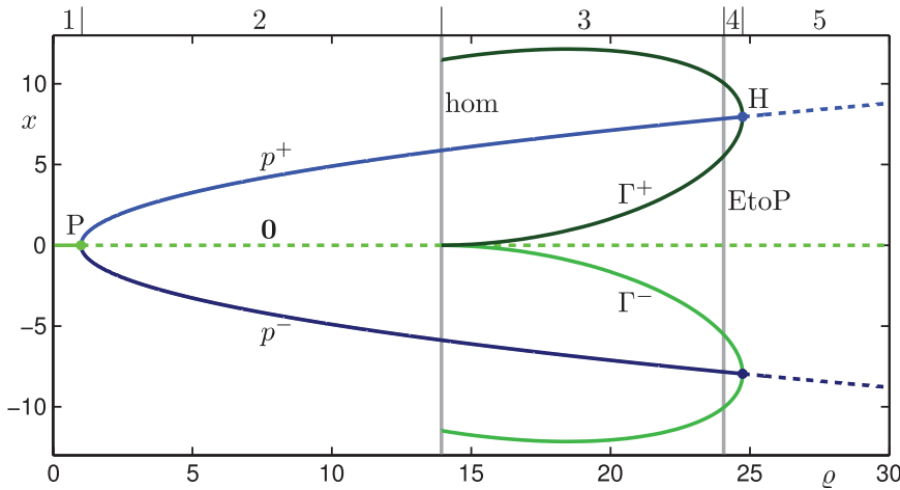


Figure 17: Bifurcation diagram of the Lorenz attractor. Source: [1]

5 TASK 5

Report on task TASK 5, Bifurcations in crowd dynamics

The SIR model is a three-dimensional system describing the process of disease spread, which is defined by Equation 9

$$\begin{aligned} \frac{dS}{dt} &= A - \delta S - \frac{\beta SI}{S + I + R} \\ \frac{dI}{dt} &= -(\delta + \nu)I - \mu(b, I)I + \frac{\beta SI}{S + I + R} \\ \frac{dR}{dt} &= \mu(b, I)I - \delta R \end{aligned} \quad (9)$$

The parameters are set as follows:

$$A = 20, \delta = 0.1, \nu = 1, \mu_0 = 10, \mu_1 = 10.45, \beta = 11.5, b = 0.01. \quad (10)$$

5.1 Vary b from 0.01 to 0.03

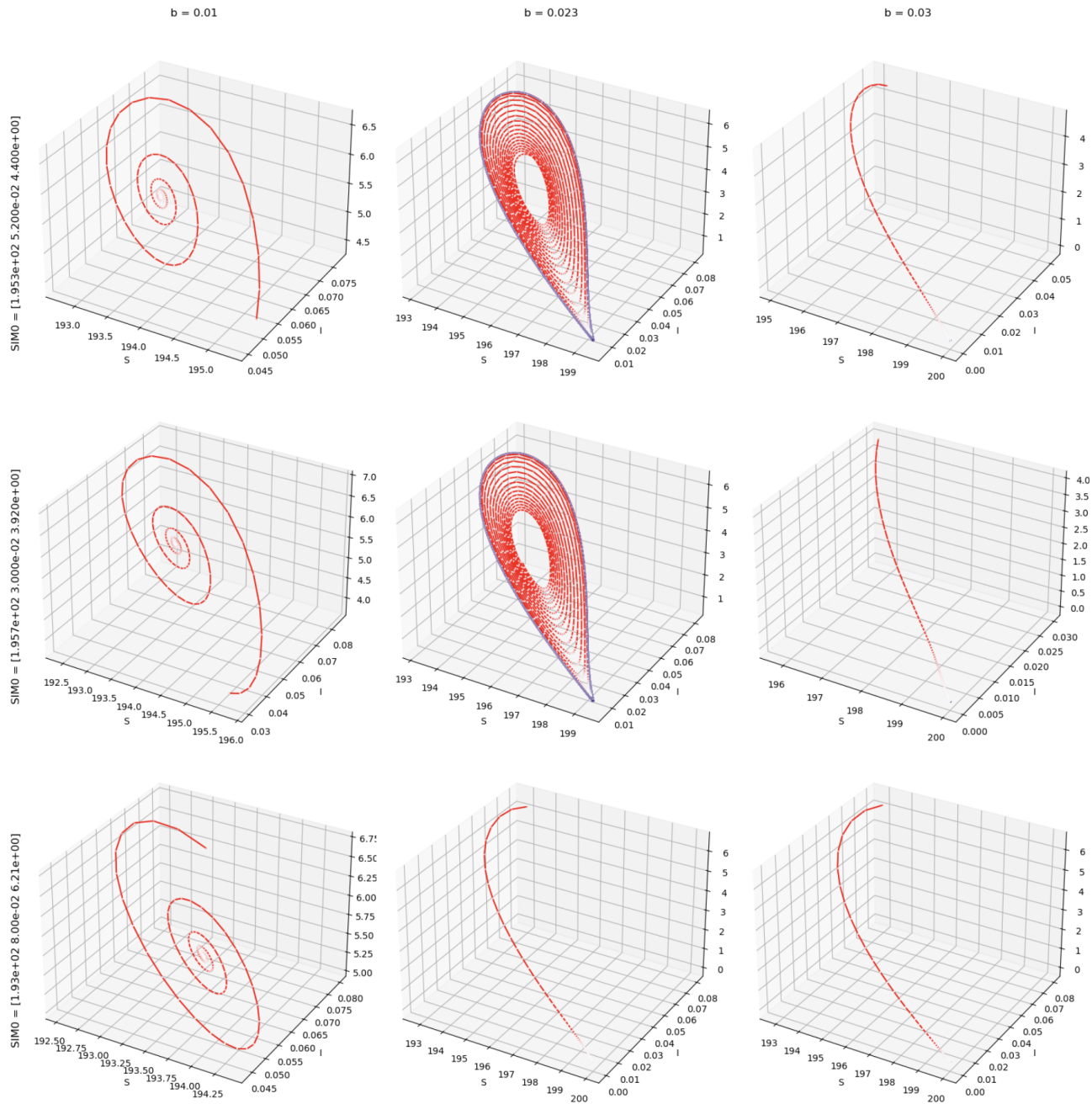
In this sub task, three different initial values of (S, I, R) : $(195.3, 0.052, 4.4)$, $(195.7, 0.03, 3.92)$ and $(193, 0.08, 6.21)$ was chosen to find the bifurcation in the SIR model. By increasing b from 0.01 to 0.03, different behaviours are found. In the first column of subplots with $b = 0.01$, all three trajectories have the same behavior of a tendency to spiral inwards to an attracting point. When the value of b increases to 0.23, the behavior of these three trajectories becomes different, as shown in the second column of subplots. The top two subplots in this column are limited in a limit cycle, while the trajectory in the bottom subplot behaves like the trajectories in the third column of subplots, converging to a equilibrium point at $(200, 0, 0)$, which is the $E_0 = (A/\delta, 0, 0)$ described in [4]. The normal form of this behavior of bifurcation is the Hopf bifurcation. This Hopf bifurcation happens at $b = 0.023$.

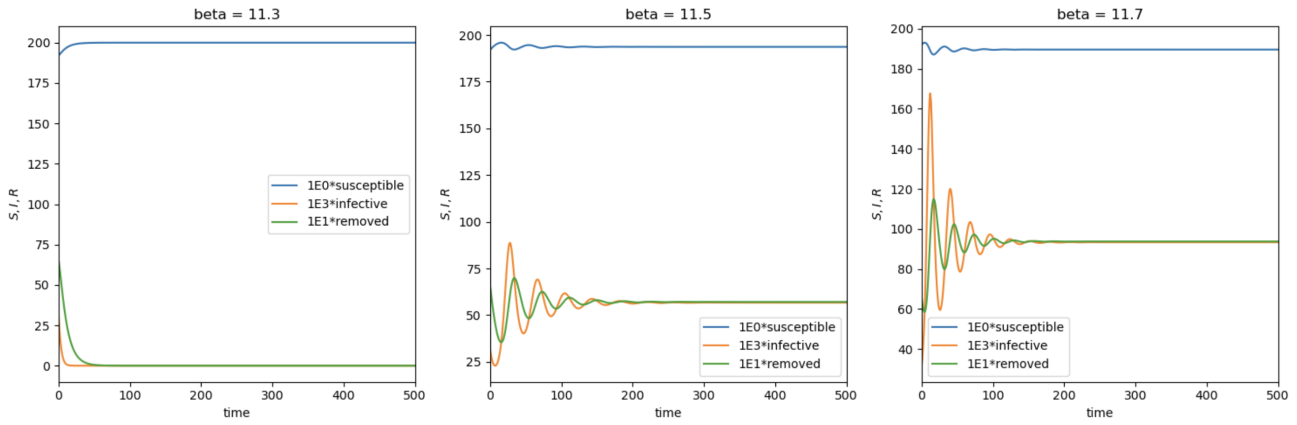
5.2 Reproduction rate and number of infective people

In 3.1 of [4], \mathbb{R}_0 is defined as:

$$\mathbb{R}_0 = \frac{\beta}{\delta + \nu + \mu_1} \quad (11)$$

β here is the average number of adequate contacts per unit time with infectious individuals. δ here is the per capita natural death rate. ν is the per capita disease-induced death rate. μ_1 is the maximum recovery rates based on the available beds.

Figure 18: Trajectory of b from 0.01 to 0.03 from different starting points

Figure 19: Infection between different values of β

So when $\mathbb{R}_0 > 1$, more people will be infected than the people recovered or dead (no matter because of disease or not), the infection will continue to spread. If $\mathbb{R}_0 < 1$, the infection tends to stop. It's illustrated with an increasing β in the Figure 19.

5.3 Attracting Node E_0

From [4], the disease free equilibrium $E_0 = (A/d, 0, 0)$ at $\mathbb{R}_0 < 1$ is an attracting node. That means the trajectories emerging around this point would converge towards this point. And the trajectories from initial values of (S, I, R) close to E_0 will also converge to E_0 . Two different situations are shown in Figure 20 and Figure 21, the first one is starting from the initial values from 5.1, the second one is starting from small disturbances.

5.4 Bonus: Another type of bifurcation

From theorem 4.1 in [4], the SIR model undergoes forward bifurcation if $\mathbb{R}_0 = 1$ and $b > \frac{A(\mu_1 - \mu_0)}{\beta(\beta - \nu)}$, considering \mathbb{R}_0 as the bifurcation parameter. In a forward bifurcation, a stable equilibrium point loses stability as a parameter is varied, and two new equilibrium points, one stable and one unstable, are created.

In this sub-task, b is set to 1.5 to keep $b > \frac{A(\mu_1 - \mu_0)}{\beta(\beta - \nu)}$. And by changing the value of β , the value of \mathbb{R}_0 is changed. The trajectories starting from $(195.3, 0.052, 4.4)$ and $(195.7, 0.03, 3.92)$ are shown in Figure 22. When \mathbb{R}_0 is smaller than 1, the trajectories converges to a stable equilibrium point $(200, 0, 0)$. But as \mathbb{R}_0 continues to increase, the former stable point loses its stability, and a new stable equilibrium appears in the following subplots.

References

- [1] Eusebius J Doedel, Bernd Krauskopf, and Hinke M Osinga. Global organization of phase space in the transition to chaos in the lorenz system. *Nonlinearity*, 28(11):R113, oct 2015.
- [2] Yuri A. Kuznetsov. *Topological Equivalence, Bifurcations, and Structural Stability of Dynamical Systems*. Springer New York, New York, NY, 2004.
- [3] Marc Roussel. *Maps: stability and bifurcation analysis*. 04 2019.
- [4] Chunhua Shan and Huaiping Zhu. Bifurcations and complex dynamics of an sir model with the impact of the number of hospital beds. *Journal of Differential Equations*, 257(5):1662–1688, sep 2014.
- [5] Eric W. Weisstein. Logistic map. <https://mathworld.wolfram.com/LogisticMap.html>, 2023. Accessed: 2024-06-03.

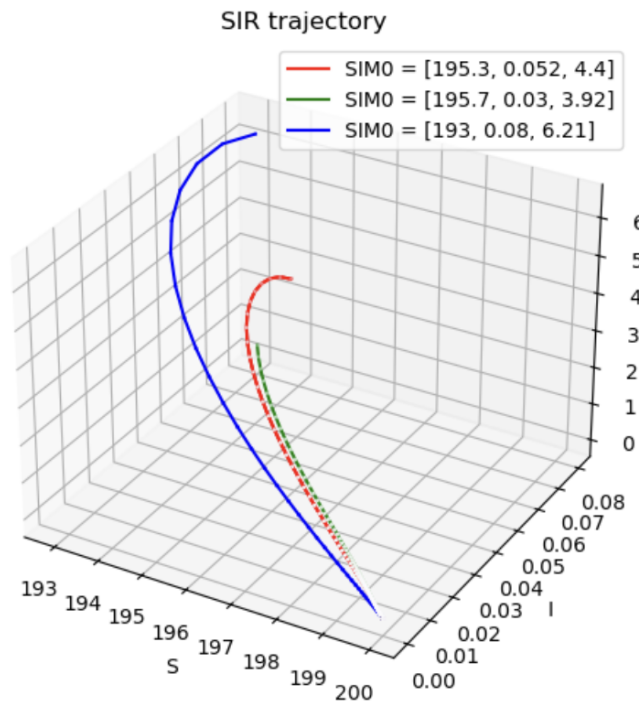
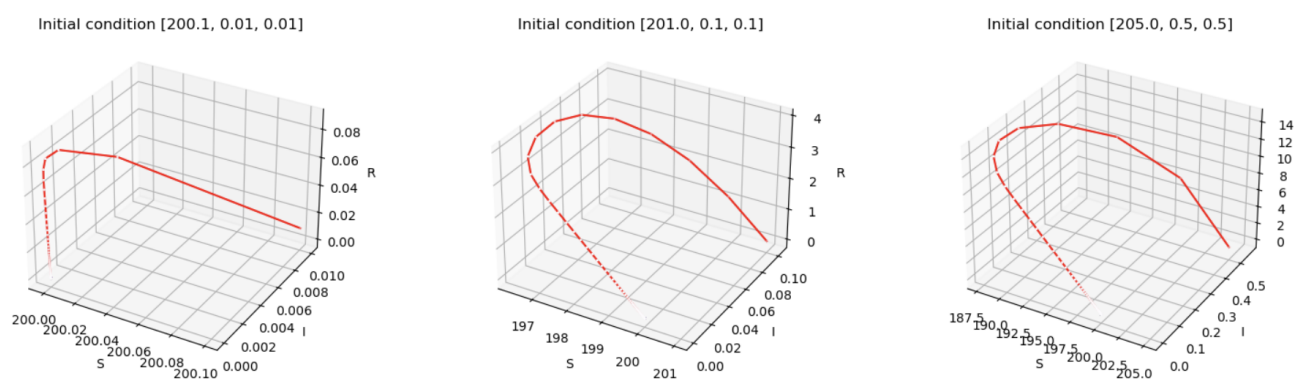


Figure 20: Trajectory of the initial values in 5.1

Figure 21: Trajectory of small disturbances around E_0

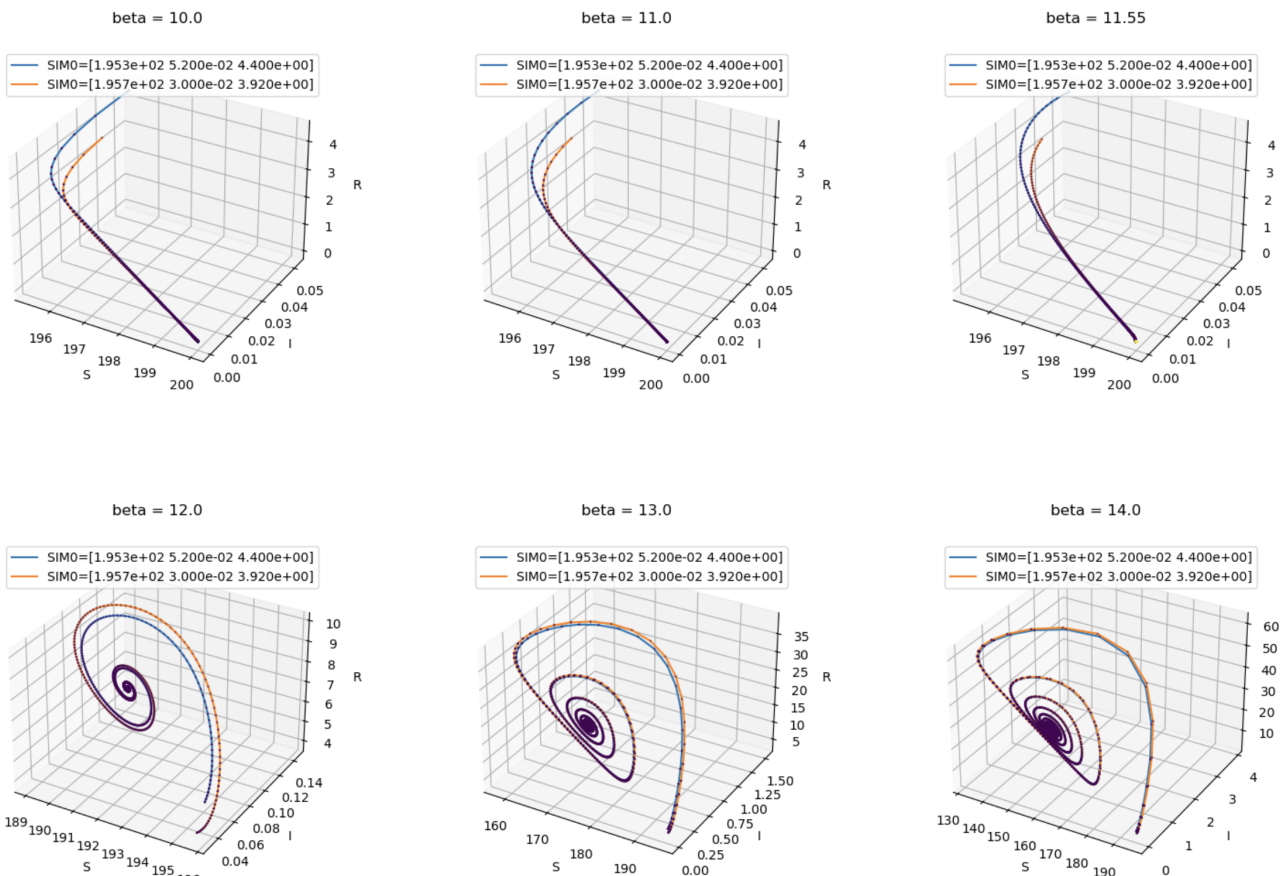


Figure 22: Trajectories of increasing β and \mathbb{R}_0 when $b > \frac{A(\mu_1 - \mu_0)}{\beta(\beta - \nu)}$